BOLLETTINO DI GEOFISICA TEORICA ED APPLICATA VOL. 43, N. 1-2, PP. 3-21; MAR.-JUN. 2002

The present day strain rate field in Italy and surrounding countries as inferred from geodetic data

A. CAPORALI, S. MARTIN and M. MASSIRONI

Dipartimento di Geologia, Paleontologia e Geofisica, Università di Padova, Italy

(Received March 13, 2001; accepted December 22, 2001)

Abstract - The EUREF 97 contribution to the ITRF97 (International Terrestrial Reference Frame 1997) includes position and velocity of permanent GPS stations in Europe for the period 1993-1998. As such, it represents the most accurate basis for analyzing the large scale plate-kinematics in the European Mediterranean region. However, defining a pattern of strain from the scattered velocity data requires the EUREF network to be locally densified with additional permanent GPS stations of quality compatible with the EUREF standards. Using the EUREF 97 velocities as a velocity datum, we have computed velocities of additional, permanent GPS stations in Italy from week 995 to week 1070 (January 1999 to July 2000). The horizontal components of the velocities have been interpolated to a regular grid of 1° x 1° size, and the components of a two dimensional, horizontal strain rate tensor were computed by numerical differentiation of the velocity components in the east and north directions, along the sides of identical triangles. The eigenvectors of a two-dimensional strain rate tensor, and their azimuth, are finally obtained at the nodes of the regular grid. When examined in the context of independent geological, seismological and geophysical knowledge, the map of the geodetically inferred strain rate field shows several interesting correlations with fault plane solutions and the geometry of pre-existing faults. Our kinematic model features an extensional regime in the Ligurian Sea and in the inner part of the Northern and Southern Apennines, and compression in the Adriatic foreland and Friuli. There is indication of compressional zones on the northern shore of Sicily. In the Channel of Sicily, the relative motion of Lampedusa and Noto results in an extension, which fits the aseismic deformation pattern in the Pantelleria Rift System. The maximum deformations occur in the Central Apennines (42° N, 12° E), with an extensional strain rate of 24 10^{-9} yr^{-1}, and in the Southern Apennines (40° N, 15° E), with an extensional strain rate of 22 10^{-9} yr^{-1}. Comparison of the

Corresponding author: A. Caporali; Dipartimento di Geologia, Paleontologia e Geofisica, Università di Padova, Via Giotto 1, 35137 Padova, Italy; phone: +39 0498272052; fax: +39 0498272070; e-mail: alessandro.caporali@unipd.it

geodetically inferred strain rate with seismic moment rates suggests that the observed deformation is mostly aseismic in the Southern Apennines, and nearly completely coseismic in the Central Apennines. About eight permanent GPS stations, located in NE Italy and Austria, indicate that north-south shortening in the Eastern Alps is 20 10^{-9} yr^{-1}. The overall sensitivity of our strain rate data, assuming a mean separation between stations of 300 km, and a random error (3σ) of the velocity of 3 mm yr^{-1}, is estimated in 14 10^{-9} yr^{-1}. In areas characterized by intense fracturing, and superposition of fault systems with different attitudes and trends, the GPS stations are too sparse to account for the short wavelength changes in stress regime. This lack of spatial resolution is evident in the Western Alps and in Sicily, where the regime clearly changes on a shorter scale than the average distance between the GPS stations in those areas. With these exceptions, we conclude that the information coming from the geodetic strain rate data fits, at least qualitatively, the broad scale neo-tectonic pattern inferred from several large scale faults, fault plane solutions of recent, shallow earthquakes, and other geophysical indicators of the stress regime.

1. Introduction

The prevalently smooth large scale stress field in continental Europe exhibits in its Alpine Mediterranean part short (~ 100 km) scale variations of tectonic regimes correlated with moderate crustal thickness and moderate to high heat flow. Several different processes take place in this limited region: opening of the Tyrrhenian basin with creation of oceanic crust, volcanism in the southern Thyrrhenian Sea, indentation of an Adriatic wedge or microplate into the Eastern Alps, flexure of the Adriatic lithosphere beneath the Apennines, development of homogeneous SW to NE thrust belts in the Dinarides, and subduction of the Ionic lithosphere beneath the Calabrian Arc. This interplay of different crustal fragments, presumably decoupled from the lithospheric mantle, is described in considerable detail in existing structural maps (Bigi et al., 1990). From a more geophysical point of view, the map of active stress in Italy has recently been considerably increased both in detail and reliability (Montone et al., 1999; Frepoli and Amato, 2000) with respect to the description given in earlier works (Udias, 1982; Mueller, 1989), or in the World Stress Map (Zoback, 1992). As pointed out by Zoback et al. (1989) and Rebai et al. (1992), for example, all the data, except in situ stress measurement, used to produce these maps are a measurement of strain rather than stress, and at varying depths. The most recent stress maps (Montone et al., 1999; Frepoli and Amato, 2000) extend the agreement between the different data types and depths which was found earlier in limited areas (Amato and Montone, 1997) to most of Italy, and it becomes desirable to test independent approaches, based upon homogeneous data sets with a reasonably good geographical distribution and, hence, spatial resolution. In the past, analyses of VLBI (Ward, 1994) and Satellite Laser Ranging data (Cenci et al., 1993; Noomen et al., 1996), particularly within the WEGENER Project (Wilson and Reinhardt, 1993), have successfully constrained present day plate-scale kinematics, but

were unable to detail an intraplate strain field, due to an insufficient distribution of continuously tracking stations and to uncertainties in the orientation of a common reference system. Today, one potentially interesting option is the high precision geodetic network EUREF (Fig. 1), which covers Europe with some 100 high quality, continuously operating stations tracking the satellites of the GPS (Global Positioning System) of the United States. EUREF contributes to the realization of the International Terrestrial Reference Frame (ITRF) (Boucher et al., 1999) by means of estimates of station coordinates and velocities, using state-of-the-art software and models of GPS observables. On behalf of EUREF, the Bundesamt fuer Kartographie und Geodaesie in Frankfurt (formerly the Astronomical Institute of the University of Bern) computes the position and velocity of the EUREF GPS stations which are, hence, defined in the most recent realization of the ITRF. The position and velocity estimates of the EUREF stations are affected by uncertainties which depend on the tracking history of the individual stations. Formal errors, in a least squares sense, are typically of the order of some millimeter and 0.1 mm yr^{-1}, respectively. Being conceived, primarily, for maintaining a geodetic reference system in Europe, the EUREF network is not optimized for studies of strain in the crust, but is potentially very attractive: if the average distance between the stations is 300 km, and the velocities are affected by a random error of 1 mm yr^{-1}, the implied uncertainty in the strain rate is less than 5 10^{-9} yr^{-1}

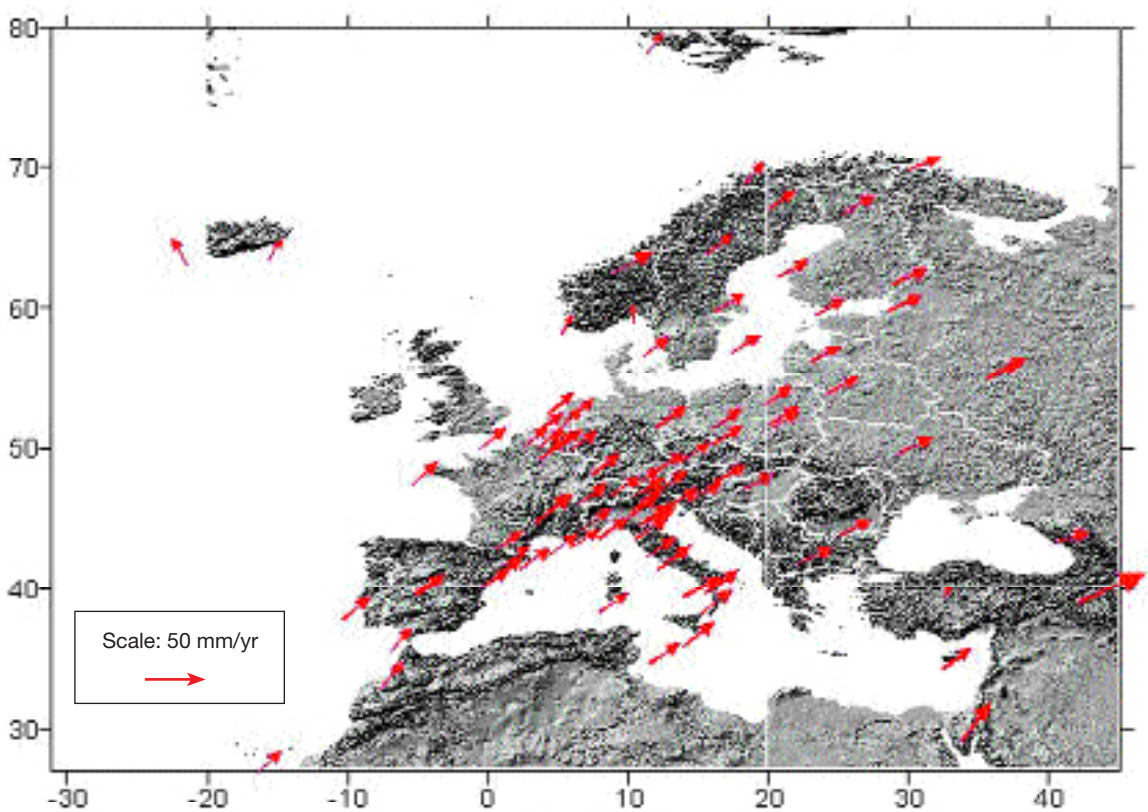

Fig. 1 - The velocities of the stations in continental Europe, according to the ITRF97 datum and its European densification EUREF 97. Topographic data base: GTOPO30 1-km elevation grid of National Oceanic and Atmospheric Administration.

at this wavelength. This is precisely the typical scale of important tectonic processes such as buoyancy or flexure of the lithosphere, which certainly play a role in the area. At present the EUREF network does not reach this density of stations, but can be locally complemented with permanent stations, for increased resolution. The EUREF Local Analysis Center at Padova University systematically processes all the permanent GPS stations in Italy which are either part of EUREF or, if not, fulfill requirements compatible with EUREF standards. Estimates of the individual velocities are periodically updated, and tied to the conventional velocity datum. The main objective of this paper is to use the velocities of this local densification of the EUREF network to identify areas of active deformation. We will attempt a comparison of the resulting pattern of deformation with the geometry of the faults, with emphasis on those dating up to Plio - Pleistocene, with focal solutions for shallow earthquakes and with the stress pattern, as derived from borehole breakouts and seismicity .

2. Data reduction

The data consist of a) the EUREF 97 set of velocities of European GPS stations of the EUREF network for the period 1993 to 1998 at the epoch 1997.0, and b) the raw GPS data files of 16 permanent GPS stations in Italy plus the Austrian station Villach (Table 1), for the period January 1999 to June 2000. The details of the computation of the ITRF97 coordinates and velocities, and of their densification EUREF 97 in Europe are described elsewhere (Boucher et al., 1999). In our weekly analysis procedure, the raw data files of the 17 GPS stations are organized in daily sessions. Processing is done with the software BERNESE 4.0 developed at the Astronomical Institute of the University of Bern (Rothacher and Mervart, 1996). Individual baselines are first processed in QIF (Quasi Iono Free) mode, and the integer ambiguities are saved. Then a network solution is computed using the L3 combination of GPS frequencies, after back-substitution of the integer ambiguities. Zenith tropospheric delays are solved every two hours with an absolute/relative a priori sigma of 5 m, and using a $\cos(z)$ mapping function, z being the zenith angle at each station of any given satellite. Elevation cutoff is at 15 degrees above the horizon. The models for phase center variations at both frequencies for each antenna type are those approved by the IGS. The program ADDNEQ (Rothacher and Mervart, 1996) is used to combine seven daily solutions into one weekly solution. The same program is used again to stack the weekly normal equation files, remove the constraints of the individual weekly solutions, constrain the velocities of selected EUREF stations to their EUREF 97 values, and solve for the horizontal velocities of the remaining stations. The EUREF stations MATE (Matera), CAGL (Cagliari), NOTO (Noto) and MEDI (Medicina), which have been all operational since over six years with combinations of GPS, Satellite Laser Ranging and Very Long Baselines techniques, were selected to orient and scale the position and velocity solution. For the EUREF stations BZRG, GENO, TORI and UNPG, the analyzed data set represents, very nearly, the totality of their available data. Consequently, the estimated velocities are in our opinion more realistic than their EUREF 97 values. Table 1 shows that the EUREF 97 velocities of these stations coincide with the predictions of the NUVEL1A NNR (DeMets et

Table 1 - Horizontal velocities (mm yr^{-1}) of permanent GPS stations in or near Italy. First column identifies the network: E = Euref, D = Densification. The first pair of velocity columns lists the velocities predicted by the model of De Mets et al. (1994). NOTO and LAMP are assumed as being in the African plate, all the remaining stations are assumed as being in the Eurasian plate. The following sub-table lists the velocities and formal uncertainties, in the least squares sense, computed for the weeks 995 - 1070 constraining the velocities of MATE, CAGL, NOTO and MEDI to their EUREF 97 values. The last sub-table similarly lists the EUREF 97 velocities. Note the close similarity of the EUREF 97 velocities of recent stations (BZRG, GENO, TORI, UNPG) to the rigid model values, caused by a priori constraints.

		NUVEL1A NNR		This solution				EUREF 97	
Net	**Station**	v_N	v_E	v_N	σ_{VN}	v_E	σ_{VE}	v_N	v_E
D	AQUI	13.38	21.34	16.25	0.09	24.67	0.07		
E	BZRG	13.71	20.49	14.76	0.06	18.31	0.04	13.70	20.44
E	CAGL	14.08	21.01	12.97	0.00	20.85	0.00	12.97	20.85
D	COSE	12.87	22.09	15.96	0.09	22.97	0.07		
E	GENO	14.08	20.36	14.74	0.06	18.39	0.05	14.11	20.38
E	LAMP	20.48	19.72	12.69	0.07	19.11	0.06	13.50	21.83
E	MATE	12.81	22.02	17.36	0.00	23.53	0.00	17.36	23.53
E	MEDI	13.66	20.81	15.32	0.00	23.12	0.00	15.32	23.12
E	NOTO	19.85	20.51	17.73	0.00	21.96	0.00	17.73	21.96
E	TORI	14.27	20.06	14.38	0.06	17.86	0.05	14.23	20.01
D	TREN	13.74	20.51	14.81	0.07	19.44	0.05		
E	UNPG	13.55	21.11	16.53	0.06	19.28	0.05	13.52	21.06
E	UPAD	13.62	20.73	17.18	0.07	18.24	0.05	15.66	21.71
E	VENE	13.62	20.73	15.22	0.06	18.67	0.04	11.26	21.81
D	VILH	13.29	20.91	17.91	0.07	19.94	0.05		
D	VLUC	13.05	21.85	14.49	0.19	21.17	0.15		

al., 1990, 1994) model. LAMP is relatively recent as a GPS station, but its velocity is well constrained by previous Mobile Satellite Laser Ranging System data. Table 2 summarizes the statistics of the solution and the adopted model. The post-fit horizontal coordinate residuals for each station are shown in Fig. 2. The scatter of the weekly estimates relative to the regression line is typically 1 mm r.m.s. (root mean square). After 6 to 8 months of continuous tracking, the estimated velocities change on average less than 1 mm yr^{-1} every time the multi-week velocity solution is updated. To better understand the level of confidence on the estimated velocities, time series of the estimated coordinates de-trended of the estimated velocity have been plotted in Fig. 3 for a well constrained station such as UPAD, and a more recent station VLUC. Taking into account that each position estimate is affected by an uncertainty of the order of a few mm,

Table 2 - Summary statistics of the solution for the period January 1999 - July 2000 in the EUREF 97 velocity datum.

Parameter	**Value**
Precise ephemeris	COD < gps-week > < day of week >. EPH
Earth orientation parameters	C04_ < year >. ERP
Antenna phase center model	PHAS_IGS.01
Total number of parameters	125,546
Number of observations	8,941,251
Number of single difference files	5,501
Sigma of single difference observation	0.0033 m

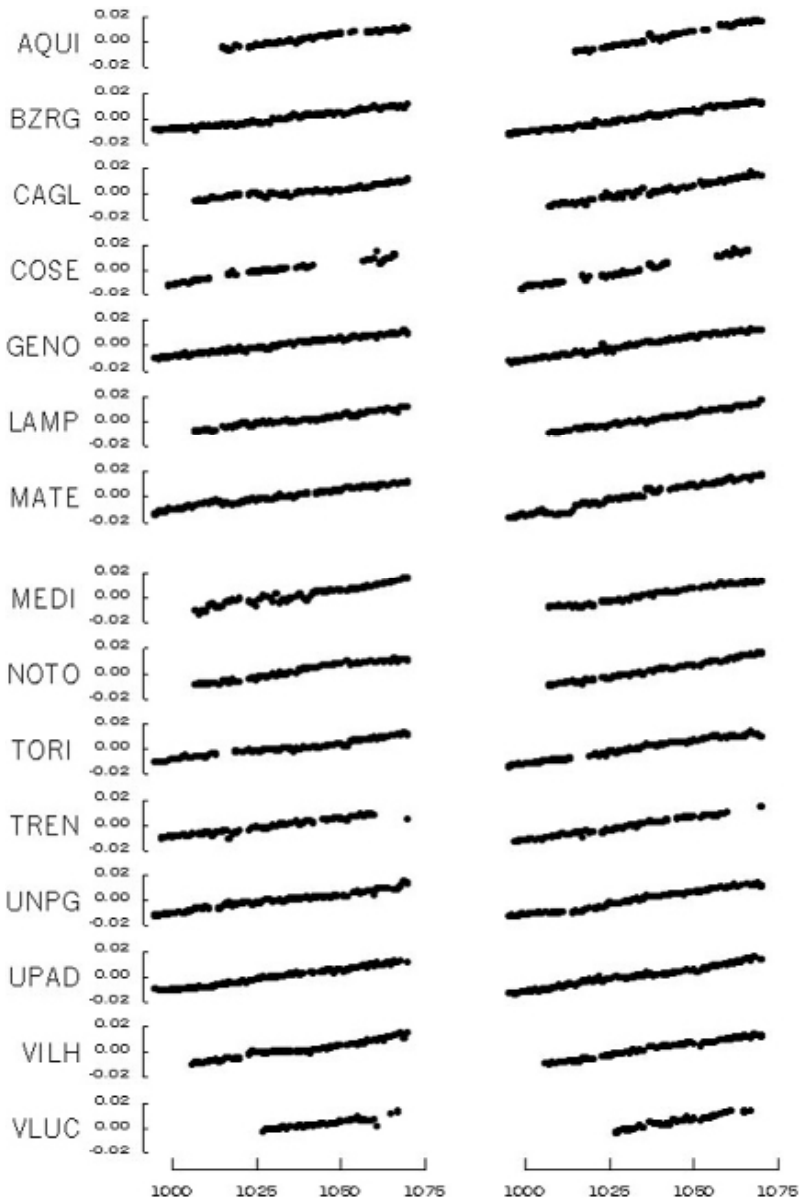

Fig. 2 - Time series of post fit residuals of the north (left) and east (right) coordinates of the Italian stations and the Austrian station Villach. Y axis units are meters; X axis units are GPS weeks; Plotting symbols are approximately 1/2 the formal error.

one concludes from the inspection of these two extreme cases that the +/- 3 mm yr^{-1} range is an acceptable estimate of the upper level of uncertainty in the horizontal velocities. The vertical velocities of the stations were, in this analysis, constrained to zero. Although, in some cases, sizable vertical motion is to be expected, the estimate of the vertical velocity is affected by a formal uncertainty 2-3 times that of the horizontal velocity. In these conditions it is meaningless to attempt a three dimensional analysis, and we decided to confine our attention to the horizontal coordinates. The computed horizontal velocities of the stations in Table 1, and the

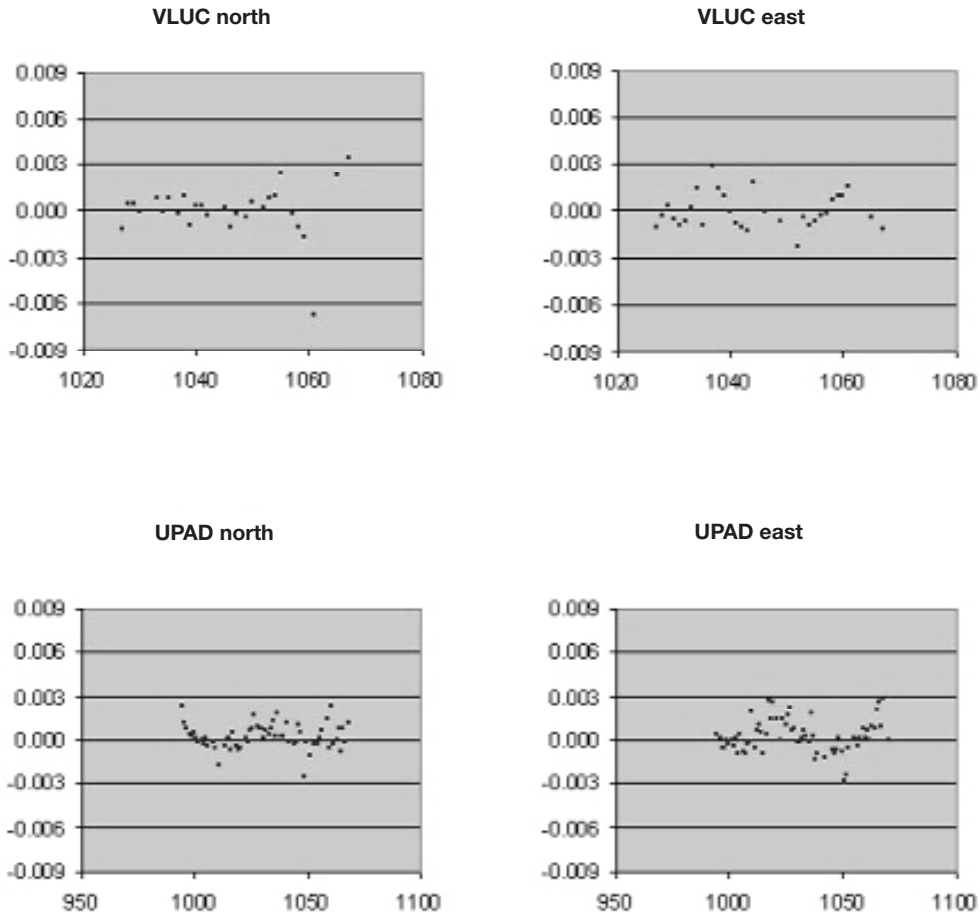

Fig. 3 - De-trended time series of VLUC (above) and UPAD (below) to exemplify that the estimated velocity is such that the probability of an event inside the +/- 3 mm belt is 99 percent or better.

EUREF 97 horizontal velocities of permanent EUREF stations, except Saint Jean des Vignes (SJDV), in neighboring countries are plotted in Fig. 4, as increments to rigid motion velocities predicted by the model NUVEL1A - NNR. The EUREF 97 velocity of SJDV was suspected to be incorrect, as it generated a large strain field which had no structural or seismological explanation. More precise values computed by the French group REGAL were used instead (Table 3) to estimate the regional strain field. The impact on the strain rate map of an erroneous velocity at one station is however an important issue, given the limited number of stations, and will be discussed in detail later on.

3. From velocities to strain rate

The available velocities are listed in Tables 1 and 3. The velocities of the remaining EUREF stations are those of the EUREF 97 or ITRF97 solution. In the computation of the velocity field, all the EUREF stations were considered. To estimate a horizontal velocity field we assume that:

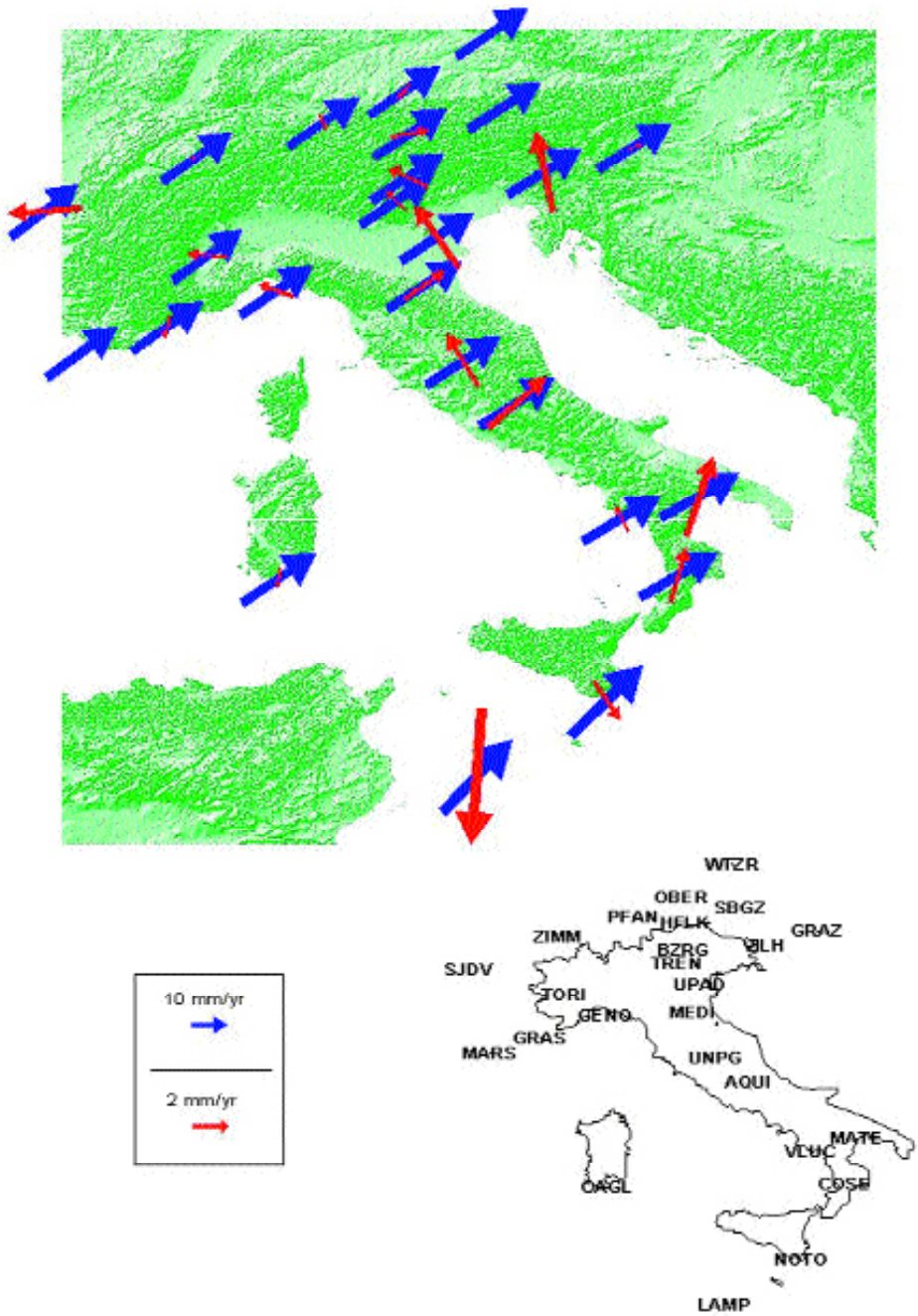

Fig. 4 - Velocities of the permanent GPS stations according to a rigid plate model NUVEL1A NNR, and their corrections, as determined from GPS data. Note the different scales for rigid plate velocities and for the additional velocities. The final velocity is the sum of the model value and the correction.

1. the selected area is a continuum at the scale of the mean distance between stations;
2. the east and north components of the horizontal velocity are statistically independent, random variables.

Assumption 1 implies that the deformation at a wavelength shorter than the distance

Table 3 - Comparison of the EUREF 97 horizontal velocities (north and east components, and absolute value and azimuth clockwise from North, of SJDV and neighbouring stations. Velocities are in mm yr^{-1}; azimuth in degrees. Note the anomalous value of the absolute velocity of SJDV leading to the local deformation in Fig. 8. The velocity used here for SJDV is the one computed by the French group Regal, based on over 2 years of data: $v_N = 14.40$, $v_E = 15.30$ (C. Vigny, private communication, July 2000).

Station	v_N	v_E	v	az
SJDV	21.21	25.18	32.93	49.91
ZIMM	13.96	19.04	23.61	53.79
MARS	14.63	19.92	24.71	53.73
GRAS	13.05	19.79	23.70	56.62
TORI	14.23	20.01	24.55	54.63

between station is negligible, and the effect of small-scale faults on the gridding process will be neglected. Assumption 2 is introduced to interpolate the two components of the velocity independently. Once the east and north components, of the horizontal velocity field have been interpolated to a regular grid, their horizontal gradients are computed by numerical differentiation across the grid. This procedure ensures that a two dimensional strain ellipse is computed at each grid point with identical triangles.

The principal sources of uncertainty of the strain rate field are a) uncertainties in the velocities of the individual stations and b) their propagation while interpolating the velocity vector from the station location to each grid node. Systematic errors in the estimated station velocities which belong to the class of residual rigid rotations will vanish by differentiation. Random errors of individual velocities, if uncorrelated, contribute to a random error of the strain rate in the form of the square root of the sum of the variances of the pairs of velocities. For two stations, 300 km apart, both with the same uncertainty (typically 3 mm yr-1 or less), the random component of the uncertainty in the strain rate is $2^{1/2}\ 10^{-8}\ yr^{-1}$, that is $14\ 10^{-9}\ yr^{-1}$. In the following, strain values above this threshold will be considered as significant.

4. The inferred strain field

The departures from velocities of a rigid motion model shown in Fig. 4 already give some idea of which kind of strain pattern may be expected. In NW Italy, the stations of GENO and TORI exhibit a westward motion which is radial to the Western Alpine Arc. The larger velocity, in the same direction, of SJDV leads to predicting some form of E-W extensional strain. In NE Italy, the departures from the rigid plate motion of the stations UPAD, TREN, BZRG and VILH suggest an indentation of an Adriatic micro-plate into continental Europe, and lead one to expect a N-S compressional strain. In particular, the BZRG and TREN velocities indicate a thrust normal to the Giudicarie lineament. The Apenninic stations MEDI and AQUI exhibit an increased velocity relative to the rigid plate model. When compared with CAGL, which moves as continental Europe, this additional velocity will result in a SW-NE extensional strain which will stretch across the Tyrrhenian sea. The motion of UNPG could reflect local deformation in a seismically very active area. The V-shaped velocity pattern of VLUC on the west side and

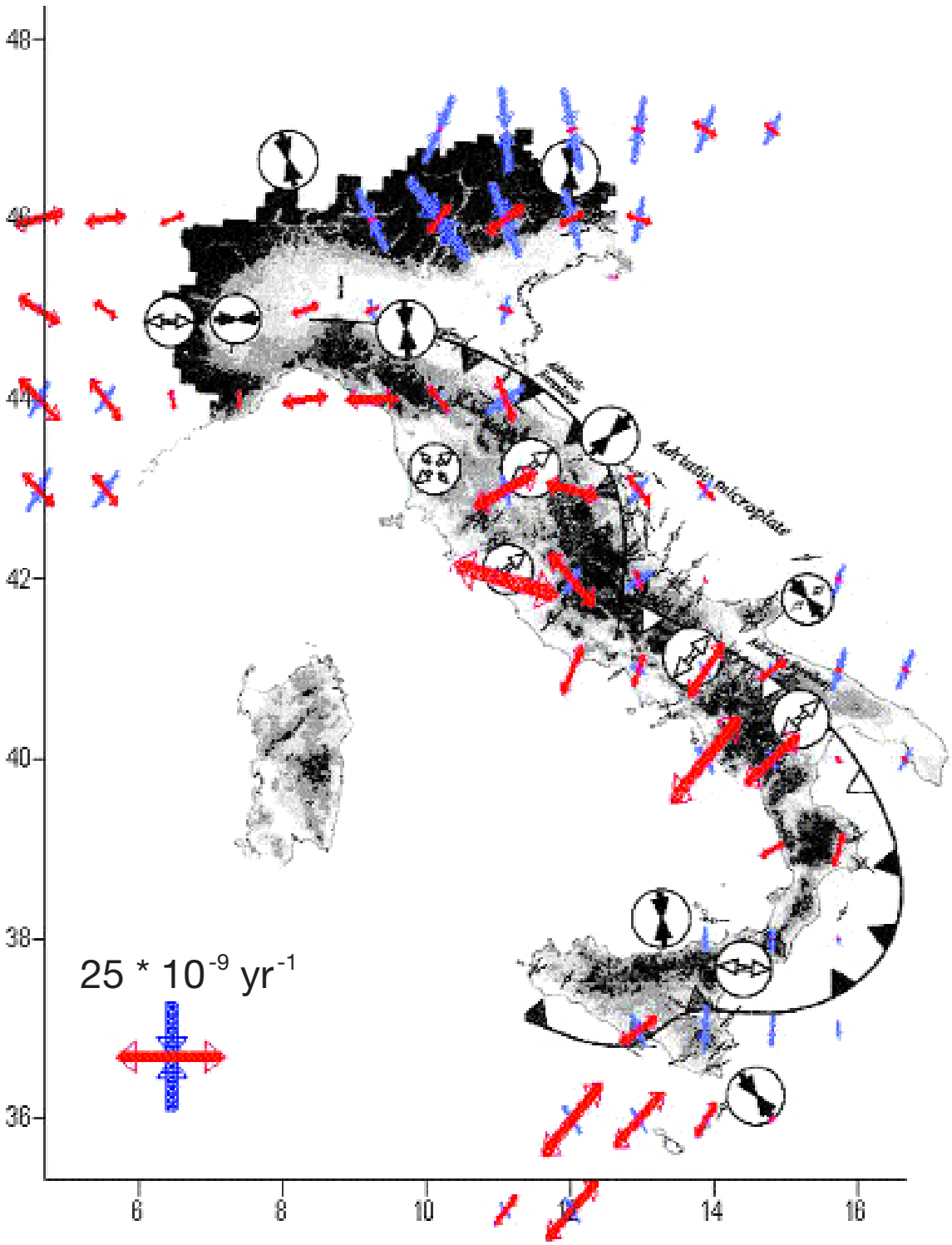

Fig. 5 - Superposition of the strain rate map with the stress map adapted from Fig. 5 of Montone et al. (1999).

COSE and MATE on the east side leads one to expect a roughly E-W extensional strain in the southern Apennines. Compression is expected across the plate boundary between Africa and Eurasia, in Central and Northern Sicily, as implied by the sharp velocity gradient. Finally, now on the African plate, the velocity gradient between NOTO and LAMP implies an extensional deformation in the Channel of Sicily.

To examine this rather complex situation from the point of view of strain rate, the compressional and extensional eigenvalues of the strain rate ellipse are plotted in Fig. 5 at the nodes of a regular grid of 1° x 1° size. The geodetically inferred strain field divides the Italian peninsula along its axis into distinct regimes:

- a small extension E-W across the Western Alps, with a maximum value of 12 10^{-9} yr^{-1} - thus below the sensitivity threshold - just north of Marseille (5°E, 44°N), with an azimuth of the extensional axis of -37° from north, clockwise; the stations MARS, GRAS, SJDV and TORI, plus the Spanish coastal stations (not shown but considered in the calculation of the velocity grid) contribute to define this pattern;
- SW flank of the Apennines, the Tyrrhenian and Ligurian Seas; the stations GENO, CAGL, UNPG, MEDI, AQUI and VLUC belong to this extensional area; the maximum values are 24 10^{-9} yr^{-1} at 12°E, 42°N, with an azimuth of the extensional axis of 102° clockwise from north, and 22 10^{-9} yr^{-1} at 15°E, 40°N, with an azimuth of the extensional axis of 47°;
- compression on the northeastern side; the stations BZRG, TREN, UPAD, VILH, GRAZ, OBER, HFLK and VENE (Venice, not shown) belong to this compressional area; the maximum values are 20 10^{-9} yr^{-1} at 11°E, 46°N, with an azimuth of the compressional axis of -44° clockwise from the north;
- some compression is visible in Sicily, north of NOTO, just below (8 10^{-9} yr^{-1}) the assumed noise level at 15°E, 37°N, with an azimuth of the compressional axis of 5°;
- extension is visible in the channel of Sicily, between NOTO and LAMP; the maximum value is 19 10^{-9} yr^{-1} at 13°E, 36°N, with an azimuth of the extensional axis of 47°.

5. A comparison of the geodetic strain with independent structural and seismic data

From the point of view of a very general tectonic setting of the whole area, the provinces indicated as under extension or compression correlate very well with zones of shallow or respectively deeper Moho isobaths, and high and, respectively, low heat flow. According to Nicolich and Dal Piaz (1991), the thickness of the crust ranges from 10 to 15 km on the Ligurian and Tyrrhenian seas, to a maximum of 25 km on the south and SW flank of the Apennines, in the regions of Toscana and Lazio. On the north and NW side, values as large as 30 to 50 km indicate a thicker crust, which is consistent with the inferred compression. Mongelli et al. (1991) likewise report heat flow values exceeding 120 mW m^{-2} in the extensional areas, and values not larger than 80 mW m^{-2} in the compressional areas.

Recently, improved maps of the horizontal stress in Italy have been published by Montone et al. (1999), and Frepoli and Amato (2000). In attempting a comparison, some caveat is necessary. First, the diversity of the data sets. The stress maps result from a combination of different types

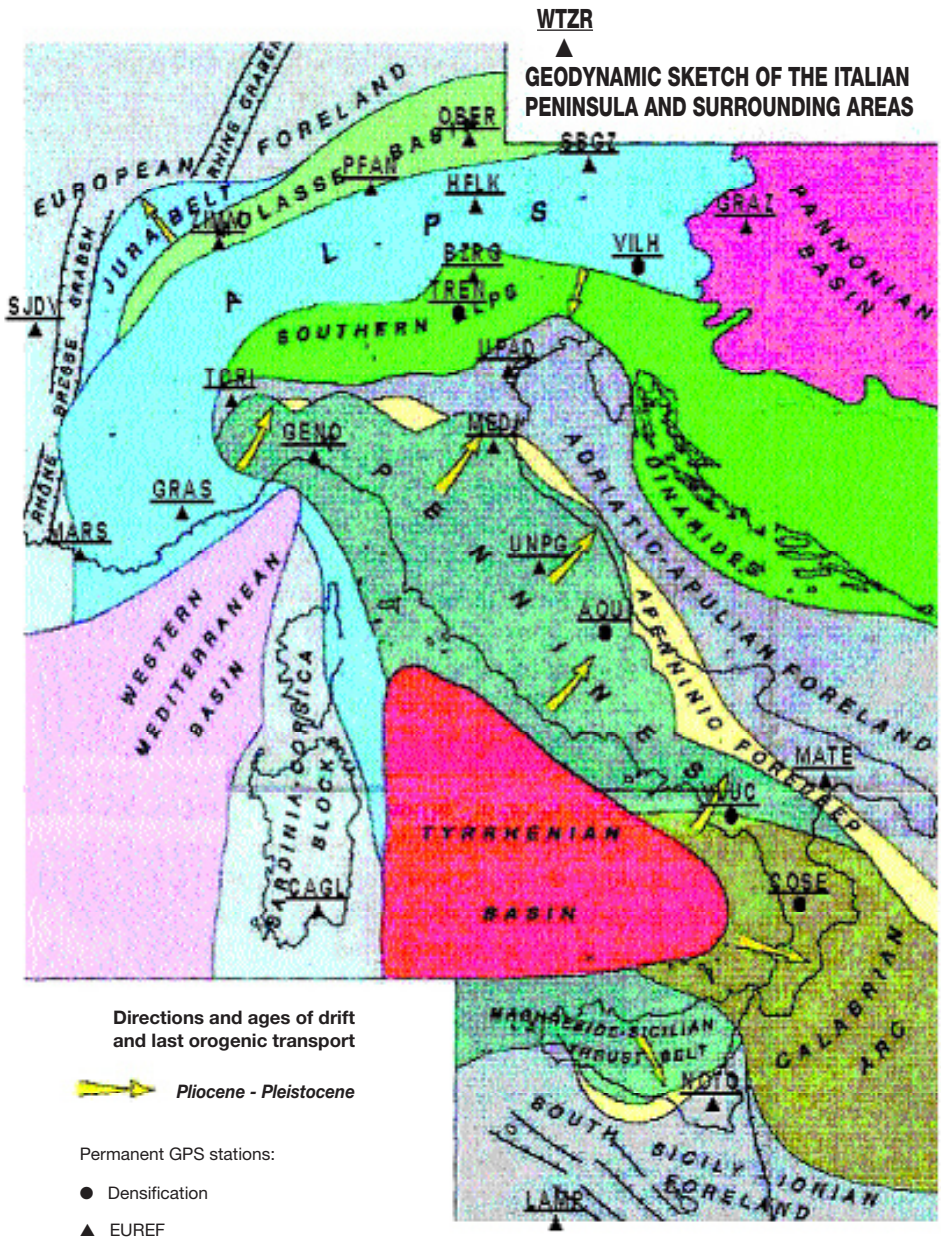

Fig. 6 - Geodynamic sketch map of Italy (adapted from Bigi et al., 1990), and the position of the permanent GPS stations.

of data: borehole breakouts give stress orientation, while fault plane solutions refer to strain. Secondly, depths and data quality may vary. Thirdly, the geographic distribution of data points is far from homogeneous, as it is for GPS stations. A comparison in a qualitative sense is therefore the best one can attempt, and the map published by Montone et al. (1999) and appearing in the background of Fig. 5 is appropriate for this purpose. The most striking areas of agreement are a) the pattern of extension along the western flank of the Central and Southern Apennines, and b) the N-S compression in NE Italy. In the Western Alps and the Western Po Plain we report no

significant deformation, whereas recent analyses of fault plane solutions (Sue et al., 1999) show a widespread extensional belt in the Western Alps bounded to the west by the external christalline massifs of Argentera, Pelvoux, Belledonne and Mont Blanc, and to the east by the Western Po Plain. Both the sandwiching eastern and western areas are under compression (Eva et al., 1998). The seismically inferred directions of extension and compression are roughly E-W. The Italian stations TORI and GENO, and the French stations SJDV and GRAS are all outside the central extensional belt. The absence in Fig. 5 of significant strain in the Western Alps is thus an example of the result of a distribution of GPS stations insufficient to sample the changes in stress regime occurring on a shorter scale (Calais et al., 2000). On the other hand, the area limited by the stations GRASS, MARS and GENO, on the Ligurian coast, includes the location of the epicenters of two earthquakes that occurred in 1989 and 1990. The focal mechanism of the two events suggested to Bethoux et al. (1992) a reactivation in compression of the Ligurian Sea, possibly driven by extrusion associated with the northward indentation of the Adriatic plate. Based on the available velocity data, Fig. 5 shows that this process, if it exists, involves a compression below the sensitivity threshold of our data.

In the nearby Eastern Alps and Friuli, we report an interesting agreement between the geodetic and the independent structural and seismic data. This area is characterized by a "cone in cone" compressional structure, consisting of two indented trapezoidal wedges, one containing the other (Bressan et al., 1998), and is bounded to the north by the Insubric line. Friuli and Slovenia still appear involved in a compressive regime historically interpreted as due to the African (or Adria) push against Europe (Renner and Slejko, 1994). This compression induced the decoupling and shortening of the Adriatic upper crust through a foreland fault-and-fold system propagating towards the Po Plain foreland. The remaining Adriatic lithosphere moved towards north, against and over the European lower plate and related orogenic belt. The region is characterized by a strong seismicity developed between 7.5 and 11 km of depth, and up to 20 km in the easternmost Friuli. Fault analysis has confirmed a N-S compression almost during earliest Pliocene, changing into NW-SE compression during the Pliocene and into a NNW-SSE at present (Castellarin et al., 1992; Mueller et al., 1992; Venturini and Fontana, 1992; Pondrelli et al., 1995; Bressan et al., 1998). The geodetic data in the NE part of Fig. 5 originate from eleven stations. With reference to Fig. 6, two stations (VENE and UPAD) belong, strictly, to the Adriatic plate, and the remaining three (TREN, BZRG and, probably only marginally, VILH) are in the Southern Alps. They all lie south of the Insubric line (with VILH marginal) and can be assumed to belong to the indenter. The indented region includes the stations OBER and PFAN in the Molasse basin, HFLK and SBGZ in the Alps, WTZR in the European foreland and GRAZ in the Pannonian Basin.

The Apenninic part of the network, in Fig. 4, consists of two stations (MATE and probably MEDI) which (Fig. 6) belong to the continuous Apenninic foredeep extending from the Po Plain to Apulia and overlying an elastic lithosphere deforming by flexure. Four additional stations (UNPG, AQUI, COSE and VLUC) belong to the inner belt. More precisely, UNPG and probably AQUI belong to the Northern-Central Apennines, VLUC to the Southern Apennines and COSE to the Calabrian Arc. The units belonging to the inner part of the belt are all under extensional regime, although fundamentally different at the lithospheric level. In the Northern

Apennines the outer transpressional zone has a σ1 horizontal and trending NE-SW (Frepoli and Amato, 1997), and the Adriatic Apulian foreland under compression. Based on instrumental and historical seismicity, Westaway (1992) estimated small, equal rates of extension and compression, ~ 0.3 mm yr^{-1} north of latitude 42.5°, that is in between AQUI (lat 42.2° N) and UNPG (lat 42.9°N). The Southern Apennines are under a larger extension, as much as 5 mm yr^{-1} south of 41°N. According to Patacca and Scandone (1987), the differential retreat of the Adriatic plate flexing beneath the northern Apennines and the Calabrian Arc was responsible for the formation of the two distinct arcs. The strain field outlined in Fig. 5 qualitatively confirms the extensional regime in the inner part of the belt. However, the behaviour of the velocity of UNPG (Fig. 4), and the consequent rapidly changing orientation of the strain in the extensional Peri Tyrrhenian zone suggest great care. This area has been considered under extension (Frepoli and Amato, 1997), but the coexistence of normal and strike slip faults, and a re-evaluation of the orientation and relative magnitude of the principal stresses has recently led to the hypothesis of a radially extending zone (Frepoli and Amato, 2000). This hypothesis can be tested with the geodetic GPS data by taking the trace of the horizontal strain rate tensor. The result is shown

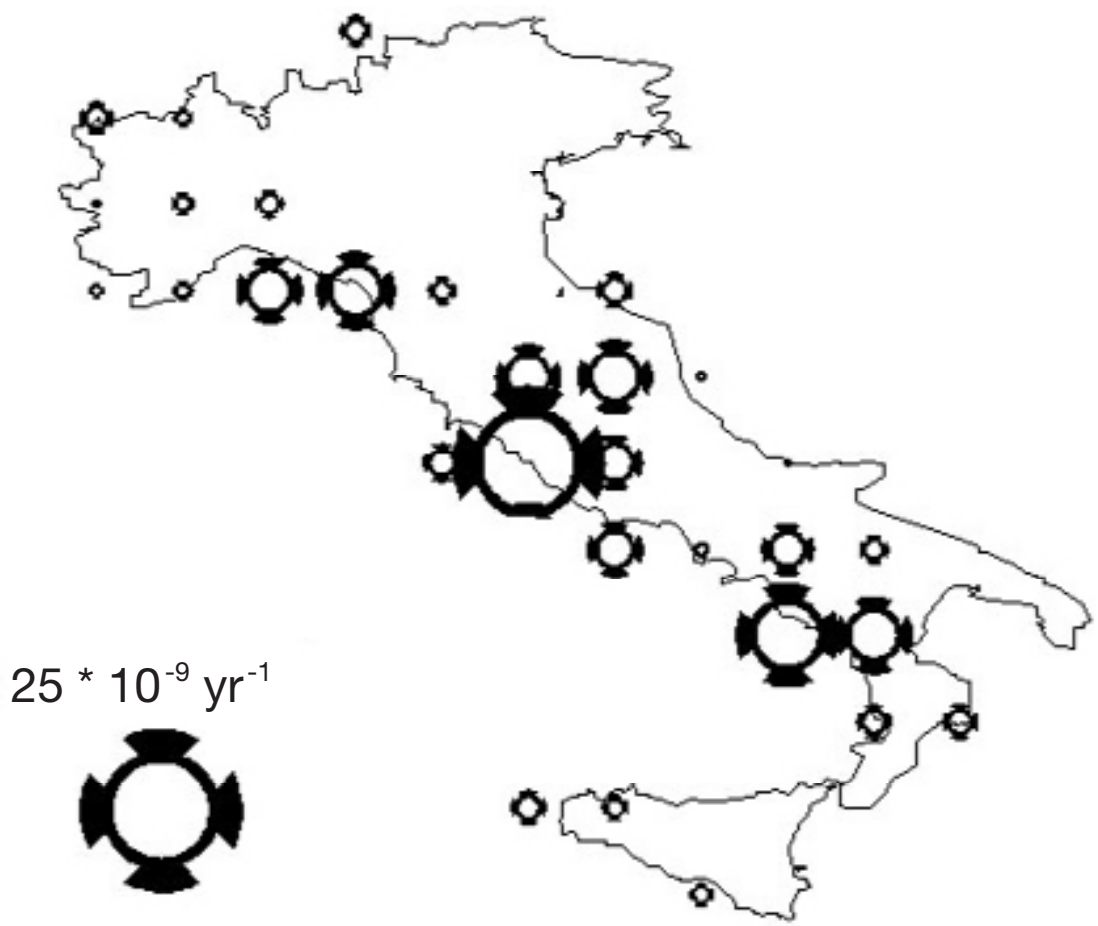

Fig. 7 - Map of the positive part of the trace of the two dimensional strain rate tensor, showing maximum radial extension in the Tuscany region.

in Fig. 7, with a qualitative indication of a maximum isotropic expansion in the Southern Peri Tyrrhenian area. In the Southern Apennines, the relative motions of the stations COSE, MATE and VLUC enable an extensional field to be identified. In the Adriatic Apulian foreland, east of MATE, there is some indication of a change to compression. It could be the consequence of a differential velocity between MATE and EUREF stations in Bulgaria, Romenia and Hungary. However, the value of the compression is below the threshold of sensitivity: new EUREF stations already operational in Macedonia and Bosnia will soon better constrain this inference.

In Sicily, the stress field is such that no single stress tensor can be computed for the entire region from seismic and borehole breakout data. Not less than four distinct areas have been identified by Frepoli and Amato (2000). On the other hand, the only GPS station NOTO is available. The situation is similar to that in the Western Alps: the scale of change of the deformation regime is considerably smaller than the average distance of the GPS stations. Our strain rate map shows a small compression defined by the NOTO and COSE stations, but this is a weakly constrained indication. Finally, the stress map reports no data on the Sicily channel, but the LAMP - NOTO baseline tends to increase in length, suggesting an extensional regime which agrees with the deformation pattern of the Pantelleria Rift System. The main grabens are the Linosa Basin, the Malta Basin and the Pantelleria Basin, with water depth up to 1700 m. Seismicity in the Channel of Sicily is low, when compared with the active convergent zones in the Sicily and Tunisia thrust faults. The few events available suggest that the present motion in the Pantelleria Rift System takes place mainly by aseismic creep (Farrugia et al., 1987).

6. The effect of local velocity anomalies

Deformation, not necessarily of tectonic origin, which is local to a GPS station, or an ill-determined velocity of a GPS station, will superimpose an anomalous velocity field to the mean, slowly varying field. The time series of the position residuals (see Figs. 2 and 3) may still be continuous, but the horizontal gradient will define an anomalous strain area. In the gridding process, the anomalous velocity of one site will affect the velocity field at nodes away from the station. It is then necessary to understand the effect of a local, anomalous velocity field in the strain map. The example of the Saint Jean des Vignes station (SJDV) is considered here. When compared with neighbouring stations (Table 3), the ITRF 97 value of the velocity of this station exhibits a value some 30% higher, and a smaller azimuth. Fig. 8 shows this anomalous velocity field, obtained by subtraction of the velocity grid with the EUREF 97 value of SJDV included and the grid computed without this station. Proceeding from the station MARS northwards, one expects a positive velocity gradient, and thus an extension roughly N-S, south of SJDV; likewise, as we move north of SJDV, one expects a compression. The resulting strain field is above the assumed sensitivity threshold and should have a well documented geophysical and geological counterpart. We are more inclined to consider the velocity of this station as still ill constrained in the EUREF 97 solution. One could also conclude that a side-benefit of the strain rate analysis is that it highlights anomalous velocities much better than time series of coordinates, for which only the repeatability can be assessed.

7. Conclusion

The strain rate inferred from GPS measurements defines a smooth pattern over Italy, which correlates with the large-scale map of Quaternary to Plio-Pleistocenic tectonics. Based on up to five years of data, from permanent satellite stations, the kinematical model features large-scale deformation patterns that are in most cases accommodated by pre-existing, large-scale faults. The agreement is less good within discrete domains characterized by intense fracturing and superposition of fault systems with different attitudes and trends, as it happens in the Western Alps, and in Sicily, where the wavelength of the deformation pattern is shorter than the mean distance between the GPS stations, resulting in poor spatial resolution. Otherwise, the agreement between the geodetically inferred strain rate and independent structural and geophysical data such as fault plane solutions or borehole breakouts is remarkable. Even more remarkable is the potential of the method, as more GPS stations contribute to densify the geodetic network. The horizontal gradient of the smoothed velocity field yields a quantitative assessment of the present day strain rate. Present seismicity and volcanism can be better

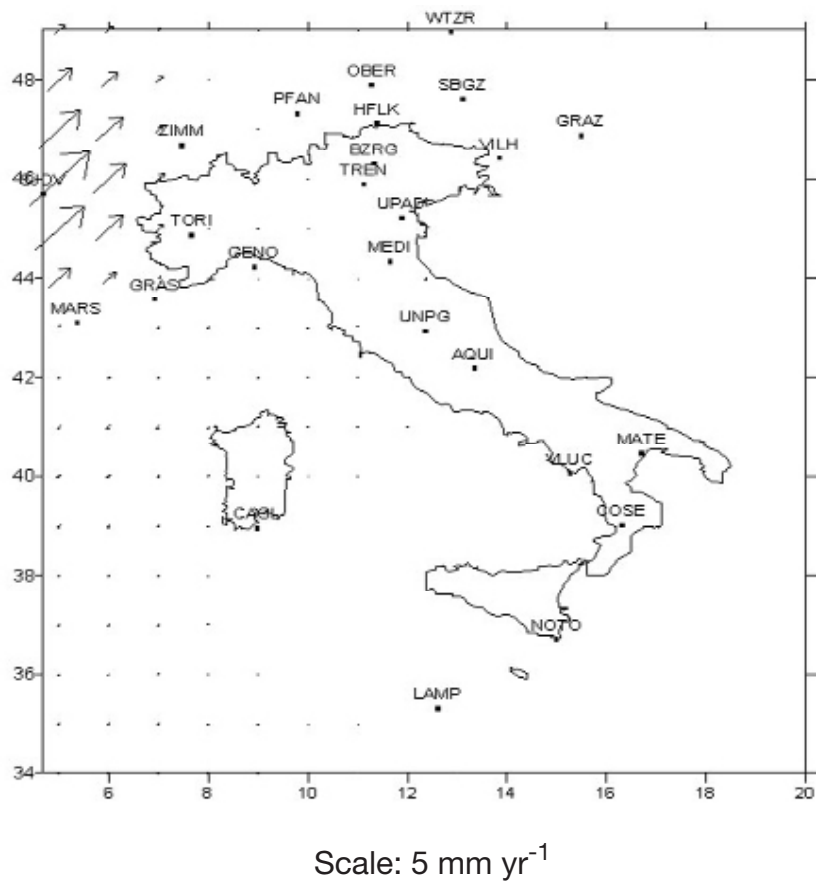

Fig. 8 - The effect on the velocity grid of the local velocity anomaly associated with the excess velocity of SJDV in the EUREF 97 velocity set. The zero, or reference, velocity field is that obtained from the ITRF97 velocities, excluding SJDV.

understood as the strain rate map becomes much more detailed and reliable. Models of lithospheric deformation in active areas, such as the Calabrian arc (Bassi et al., 1998; Mantovani et al. 1997, 2000) can be constrained by assigning the strain pattern to the brittle upper crust as a boundary condition. Our directly measured strain rates can be useful when analyzing the relationship between seismic moment rates and tectonic moment rates. In a region with along strike length L and average dip of the faults δ, the relative velocity for co-seismic deformation can be estimated from the equation (Aki and Richards, 1980)

$$\nu = \frac{M_0 sin\,(2\delta)}{2\mu HLt} \tag{1}$$

where M_0 is the sum of the scalar seismic moment, H (~ 10 km) is the thickness of the brittle layer, μ (~ 30 GPa) is the shear modulus and t is the integration time over several earthquakes. Thus, comparing the geodetically inferred strain with the strain inferred from coseismic deformation can help in constraining the amount of deformation which is accommodated aseismically. Knowing the variation of the velocity from one grid node to the next can finally help in constraining the amount of tapering of the velocity field in the deformation area. For example (Westaway, 1992), in the Southern Apennines ($L \sim 400$ km, $\delta \sim 45°$) an upper limit for the cumulative seismic moment is $M_0 = 40\ 10^{18}$ Nm in the past 350 years, which corresponds to 0.5 mm yr^{-1}. Kinematic estimates give a total velocity of 5 mm yr^{-1} since 0.7 Ma near 41°N latitude, which would imply a predominance (~ 90%) of aseismic relative motion in the total velocity. Our data (Table 1) give a relative velocity of MATE and VLUC of 3.7 mm yr^{-1}. Considering that the VLUC velocity is as yet only marginally constrained by the time series in Fig. 2, and that the uncertainties in Westaway's estimates are probably as large as the geodetic GPS figures, one can speak of qualitative agreement, at this time. Further north, in the Central Apennines, we report similar or smaller strain rates, but the cumulative seismic moments are here about ten times larger than in the Southern Apennines. Even allowing for higher dip angles in Eq. 1, this fact lends support to the hypothesis of aseismic deformation being nearly negligible in the Central Apennines, and that the ~ 2 mm yr^{-1} relative velocities have a seismic origin.

References

Aki K. and Richards P.G.; 1980: *Quantitative seismology: theory and methods*. Freeman, San Francisco, California, 932 pp.

Amato A. and Montone P.; 1997: *Present - day stress field and active tectonics in southern peninsular Italy*. Geophys. J. Int., **130**, 519-534.

Bassi G., Sabadini R. and Rebai S.; 1998: *Modern tectonic regime in the Tyrrhenian area: observations and models*. Geophys. J. Int., **129**, 330-346.

Bethoux N., Frechet J., Guyoton F., Thouvenot F., Cattaneo M., Eva C., Nicolas M. and Granet M.; 1992: *A closing Ligurian sea?*. Pageoph, **139**, 179-194.

Bigi G., Cosentino D., Parotto M., Sartori R. and Scandone P.; 1990: *Structural model of Italy. Sheet n. 1*. In:

Castellarin A., Coli M., Dal Piaz G.V., Sartori R., Scandone P. and Vai G.B. (eds), Structural model of Italy, CNR, progetto finalizzato Geodinamica, Roma.

Boucher C., Altamimi Z. and Sillard P.; 1999: *The 1997 International Terrestrial Reference Frame (ITRF97)*. IERS Technical Note n. 27. Observatoire de Paris, 191 pp.

Bressan G., Snidarcig A. and Venturini C.; 1998: *Present state of tectonic stress of the Friuli area (Eastern Southern Alps)*. Tectonophysics, **292**, 211-227.

Calais E., Galisson L., Stéphan J.-F., Delteil J., Deverchère J., Larroque C., Mercier de Lépinay B., Popoff M. and Sosson M.; 2000: *Crustal strain in the Southern Alps, France, 1948-1998*. Tectonophysics, **319**, 1-17.

Castellarin A., Cantelli L., Fesce A.M., Mercier J.L., Picotti V., Pini G.A., Prosser G. and Selli L.; 1992: *Alpine compressional tectonics in the Southern Alps. Relationships with the N-Apennines*. Annales Tectonicæ, **6**, 62-94.

Cenci A., Fermi M., Sciarretta C., Devoti R. and Caporali A.; 1993: *Tectonic motion in the Mediterranean Area from Laser Ranging to LAGEOS*. In: Smith D.E. and Turcotte D.L. (eds), Contributions of Space Geodesy, Crustal Dynamics, Geodynamics Series **23**, American Geophysical Union, Washington D.C., pp. 347-358.

De Mets C., Gordon R.G., Argus D.F. and Stein S.; 1990: *Current plate motions*. Geophys. J. Int., **101**, 425-478.

De Mets C., Gordon R.G., Argus D.F. and Stein S.; 1994: *Effect of recent revisions to the geomagnetic reversal time scale on estimates of current plate motions*. Geophys. Res. Lett., **21**, 2191-2194.

Eva E., Pastore S. and Deichmann N.; 1998: *Evidence for ongoing extensional deformation in the Western Swiss Alps and thrust-faulting in the SouthWestern Alpine foreland*. J. Geodyn, **26**, 27-43.

Farrugia P., Apopei I. and Bonjer K.P.; 1987: *Observations of seismicity of the Sicily channel*. Mem. Soc. Geol. It., **38**, 329-340.

Frepoli A. and Amato A.; 1997: *Contemporaneous extension and compression in the northern Apennines from earthquake fault plane solutions*. Geophys. J. Int., **129**, 368-388.

Frepoli A. and Amato A.; 2000: *Spatial variation in stresses in peninsular Italy and Sicily from background seismicity*. Tectonophysics, **317**, 109-124.

Mantovani E., Albarello D., Tamburelli C., Babbucci D. and Viti M.; 1997: *Plate Convergence, crustal delamination, extrusion tectonics and minimization of shortening work as main controlling factors of the recent Mediterranean deformation pattern*. Ann. Geof. **40**, 611-643.

Mantovani E., Viti M., Albarello D., Tamburelli C., Babbucci D. and Cenni N.; 2000: *Role of kinematically induced horizontal forces in Mediterranean tectonics: insight from numerical modeling*. J. Geodyn. **30**, 287-320.

Mongelli F., Zito G., Della Vedova B., Pellis G., Squarci P. and Taffi L.; 1991: *Geothermal regime in Italy and surrounding areas*. In: Cermak V. and Rybach L. (eds), Exploration of the Deep Continental Crust, Springer Verlag, Berlin.

Montone P., Amato A. and Pondrelli S.; 1999: *Active stress map of Italy*. J. Geophys. Res., **104**, 25595-25610.

Mueller B., Zoback M.L., Fuchs K., Mstin L., Gregersen S., Pavoni N., Stephansson O. and Ljunggren C.; 1992: *Regional patterns of tectonic stress in Europe*. J. Geophys. Res., **97**, 11783-11803.

Mueller St.; 1989: *Deep-reaching geodynamic processes in the alps, in alpine Tectonics*. In: Coward M.P., Dietrich D. and Park R.G. (eds), Spec. Publ. Geol. Soc. London, **45**, pp. 303-328.

Nicolich R. and dal Piaz G.V.; 1991: *Isobate della Moho in Italia*. In: Castellarin A., Coli M.; Dal Piaz G.V., Sartori R., Scandone P. and Vai G.B. (eds), Structural Model of Italy, 6 Sheets, 1:500,000, CNR Progetto finalizzato Geodinamica, Roma.

Noomen R., Sprinter T.A., Ambrosius B.A.C., Herzberger K., Kuijper D.C., Mets G.J., Overgaaw B. and Wakker K.F.; 1996: *Crustal deformation in the Mediterranean area computed from SLR and GPS observations*. J. Geodyn, **21**, 73-96.

Patacca E. and Scandone P.; 1987: *Post Tortonian mountain building in the Apennines: the role of the passive sinking of a relic lithospheric slab*. In: Boriani A., Bonafede M., Picardo G.B. and Vai G.B. (eds), The Lithosphere in Italy: advances in Earth Science research, Accademia Nazionale dei Lincei, Mid Term Conference, Rome 5-6 May 1987, pp.157-176.

Pondrelli S., Morelli A. and Boschi E.; 1995: *Seismic deformation in the Mediterranean area estimated by moment tensor summation*. Geophys. J. Int., **122**, 938-952.

Rebai S., Philip H. and Taboada A.; 1992: *Modern tectonic stress field in the Mediterranean region: evidence for variation in stress directions at different scales*. Geophys. J. Int., **110**, 106-140.

Renner G. and Slejko D.; 1994: *Some comments on the seismicity of the Adriatic region*. Boll. Geof. Teor. Appl., **36**, 141-144.

Rothacher M. and Mervart L. (eds); 1996: *Bernese GPS software version 4.0,* Astronomical Institute of the University of Bern. 418 pp.

Sue C., Thouvenot F., Fréchet J. and Tricart P.; 1999: *Widespread extension in the core of the western Alps revealed by earthquake analysis*. J. Geophys. Res. **104**, 25611-25622.

Udias A.; 1982: *Seismicity and seismotectonic stress-field in the Alpine Mediterranean region, in Alpine-Mediterranean geodynamics*. In: Berckhemer H. and Hsu K. (eds), AGU-GSA Geodynamics Series, **7**, pp. 75-82.

Venturini C. and Fontana C.; 1992: *The Neoalpine phase in the Carnic Alps: secondary E-W compressions*. Studi Geologici Camerti volume speciale CROP **1-1A**, 271-274.

Ward S.N.; 1994: *Constraints on the seismotectonics of the Central Mediterranean sea from Very Long Baseline Interferometry*. Geophys. J. Int., **117**, 441-452.

Westaway R.; 1992: *Seismic moment summation for historical earthquakes in Italy: Tectonic implications*. J. Geophys. Res. **97**, 15437-15464.

Wilson P. and Reinhardt E.; 1993: *The WEGENER-Medlas Project: preliminary results on the determination of the geokinematics of the Eastern Mediterranean*. In: Smith D.E. and Turcotte D.L. (eds), Contributions of Space Geodesy: Crustal Dynamics. Geodynamics Series, **23**, American Geophysical Union, Washington D.C., pp. 299-309.

Zoback M.L. et al. (29 authors); 1989: *Global patterns of tectonic stress*. Nature, **341**, 291-298.

Zoback M.L.; 1992: *First and second order patterns of stress in the lithosphere: The World Stress Map Project*. J. Geophys. Res., **97**, 11703-11728.